Journal of Power Sources 196 (2011) 7313–7317

Contents lists available at ScienceDirect

Journal of Power Sources

journal homepage: www.elsevier.com/locate/jpowsour

Short communication

Effects of chromium poisoning on the long-term oxygen exchange kinetics of the solid oxide fuel cell cathode materials $La_{0.6}Sr_{0.4}CoO_3$ and Nd_2NiO_4

Min Yang, Edith Bucher, Werner Sitte*

University of Leoben, Franz-Josef-Strasse 18, A-8700 Leoben, Austria

ARTICLE INFO

Article history:
Received 26 July 2010
Received in revised form 20 October 2010
Accepted 21 October 2010
Available online 30 October 2010

Keywords:
Solid oxide fuel cells
Cathode materials
Strontium segregation
Chromium poisoning
Oxygen exchange kinetics

ABSTRACT

The influence of chromium poisoning on the long-term stability of the oxygen exchange kinetics of the promising IT-SOFC cathode materials $La_{0.6}Sr_{0.4}CoO_{3-\delta}$ (LSC) and $Nd_2NiO_{4+\delta}$ (NDN) is investigated in-situ by dc-conductivity relaxation experiments. The as-prepared LSC and NDN samples show high chemical oxygen surface exchange coefficients k_{chem}. After the deposition of a 10 nm thick Cr-layer onto the surface, k_{chem} of LSC decreases to 50% of the initial value. Additional chromium deposition of 20 nm on LSC leads to a further decrease of k_{chem} to 27% of the initial value. In contrast, the effect of a 10 nm thick Cr-layer on k_{chem} of NDN is negligible. Even with additional 20 nm of chromium and a total testing time of 1750 h, the nickelate retains a k_{chem} of 60% of the initial value. X-ray photoelectron spectroscopy (XPS) of the degraded. LSC shows a significantly altered surface cation composition with Sr-enrichment down to 30 nm depth while XPS analysis of the degraded NDN reveals a thin surface zone of approximately 30 nm containing nickel and chromium. In contrast to LSC, the changes in the surface composition of NDN due to Cr-poisoning ultimately had only a minor influence on the surface exchange properties.

1. Introduction

Intermediate-temperature solid oxide fuel cells (IT-SOFCs) are of great interest as highly efficient power generation systems with the advantage that – at operating temperatures between 600 and 750 °C – cost effective metallic alloys (stainless steels) can be used as interconnects. However, these systems also require cathode materials with excellent catalytic activity for oxygen reduction at lower temperatures. During the last two decades, mixed electronic–ionic conducting transition metal perovskites were favored as the most promising cathode candidates [1–6]. In fact, excellent oxygen exchange properties resulting in high cell performances and low area specific resistance (ASR) were reported, e.g. for $(La,Sr)CoO_{3-\delta}$ [7–9]. However, the high content of alkaline earth elements such as Sr, which is a prerequisite for the high oxygen non-stoichiometries and fast oxygen diffusivity of these perovskites, has been shown to be a considerable source of degradation, particularly during long-term operation in real atmospheres [10–14].

More recently, oxygen hyper-stoichiometric nickelates such as $Ln_2NiO_{4+\delta}$ (Ln = La, Pr, Nd) have been proposed as alternative Sr-free cathodes [15–17]. The K_2NiF_4-structure, i.e. the first member of the Ruddlesden-Popper series $A_{n+1}B_nO_{3n+1}$, can be described as a stacking of perovskite-like layers alternating with rock salt-like layers along the *c*-direction [18]. By means of the incorporation of excess oxygen into the rock salt layers, high oxygen non-stoichiometry (excess) is obtained without the need for A-site substitution [19–21]. As one of the most promising cathode materials of this series, $Nd_2NiO_{4+\delta}$ was shown to exhibit excellent performance down to 600 °C [15,17,22,23]. However, long-term studies on the stability of the oxygen exchange kinetics of these new materials are scarce. With respect to the targeted application in IT-SOFCs with metallic interconnects over timescales of 5000 h (mobile systems) to 40,000 h (stationary systems), the failure mechanism of Cr-poisoning is of special importance. The degradation induced by the gas-phase transport of volatile Cr-species originating from the metallic interconnects and their reaction with the cathode is currently one of the main issues of IT-SOFC research and development [5,24–28]. Even though sophisticated protection layers for the interconnects have recently been developed [29–33], Cr-poisoning remains a major obstacle for the market introduction of IT-SOFCs with acceptable life-spans.

In the present study, the Cr-induced degradation of $La_{0.6}Sr_{0.4}CoO_{3-\delta}$ (LSC) and $Nd_2NiO_{4+\delta}$ (NDN) is investigated under well-defined conditions. The process of Cr-poisoning is simulated by evaporating Cr-layers of increasing thickness directly onto the sample surfaces. Using the electrical dc-conductivity relaxation technique, the resulting changes of the chemical surface

* Corresponding author at: Department of General, Analytical and Physical Chemistry, Franz-Josef-Strasse 18, 8700 Leoben, Austria.
Tel.: +43 3842 402 4800; fax: +43 3842 402 4802.
E-mail address: sitte@unileoben.ac.at (W. Sitte).

0378-7753/$ – see front matter © 2010 Elsevier B.V. All rights reserved.
doi:10.1016/j.jpowsour.2010.10.064

oxygen exchange coefficient (k_{chem}) are monitored in-situ as a function of time. XPS-depth profiling is applied for the detailed analysis of the compositional changes of both the surface and the bulk regions. The combination of these methods allows for a deeper insight into the extent and origin of chromium poisoning of Sr-containing vs. Sr-free cathode materials.

It should be mentioned that the present experimental approach may not exactly mimic the Cr-poisoning processes taking place in an actual SOFC cathode. However, the main advantages of the applied method are that chromium poisoning of new SOFC cathodes can be studied (and compared) by depositing Cr-layers of exact thicknesses onto the surfaces of compact samples, thus avoiding undefined transport rates of Cr from an external source, followed by in-situ monitoring the oxygen reduction reaction in combination with studies of the elemental depth profiles of the surface near region. Additionally, due to the absence of a solid electrolyte, any electrode–electrolyte side reactions can be avoided. The paper should also demonstrate that the thicknesses of these Cr-layers need to be in the nanometer range in order to be able to evaluate the influence of chromium in the surface-near region and to get a first impression of the extent of Cr-diffusion within the 1000+ h range, also at temperatures as low as 600 °C.

2. Experimental

2.1. Sample preparation

Commercially available $La_{0.6}Sr_{0.4}CoO_{3-\delta}$ powder (Praxair Inc.) was uniaxially pressed into a rod and sintered at 1200 °C for 4 h in air to form a dense pellet with a thickness of 26 mm, a diameter of 8 mm and a density of 98%. $Nd_2NiO_{4+\delta}$ powder was synthesized by the polyacrylamide gel route as described elsewhere [17,34]. Uniaxial pressing and sintering at 1350 °C for 4 h gave a cylindrical sample 15 mm in diameter and 7 mm in thickness with a density of 98%. From these tablets, thin squares with areas of about 6 mm × 6 mm were cut using a diamond wire saw. The LSC and NDN slices were ground and polished on polymer-embedded diamond lapping films to final thicknesses of 171 and 182 μm, respectively. Electrical contacts were established by means of gold wires, attached to the four corners of the ceramic samples with gold paste (Metalor).

2.2. Electrical conductivity relaxation measurements

The oxygen exchange kinetics was investigated at 600 °C under conditions close to equilibrium by applying small changes of the oxygen partial pressure in the interval $0.10 \leq p(O_2)/\text{bar} \leq 0.15$. The gas flow rate amounted to 2 $dm^3\ h^{-1}$. The electrical conductivity response of the samples was evaluated with respect to the chemical oxygen surface exchange coefficient (k_{chem}) by nonlinear least-squares fits to the adequate diffusion model [35]. Further details of the setup of 4-point dc-conductivity relaxation experiments (CR) can be found elsewhere [36]. As a consequence of the low thickness of the samples, the kinetics was rate-controlled by the surface oxygen exchange process and – except for a few cases – k_{chem} was able to be obtained as a single fit parameter with high precision.

In order to study the effects of chromium poisoning on the kinetic parameters under well-defined conditions, Cr-layers of 10–30 nm total thickness were evaporated in two steps onto both surfaces of the LSC and NDN samples using a MSC 010 multi control system coupled with an MED 020 coating system from BAL-TEC (Leica) with a Cr-target (99.996% purity, Sigma–Aldrich). The chromium layers were evaporated onto the sample surfaces including the gold contacts at the corners of the samples. However, the thin Cr-layers on top of the macroscopic gold contacts are not expected to have any significant influence on the electrical conductivity relaxation measurements.

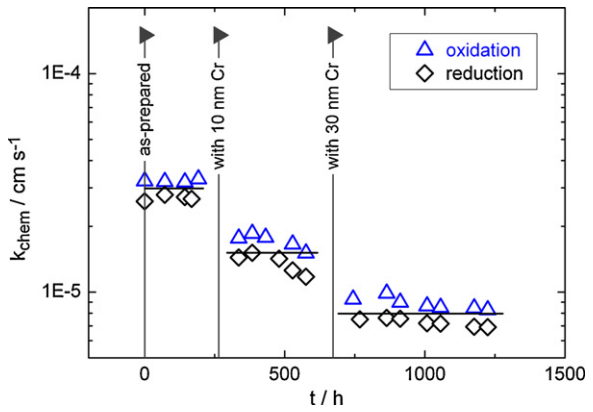

Fig. 1. Decrease of the chemical oxygen surface exchange coefficient k_{chem} of LSC due to chromium poisoning at 600 °C. Data of the fresh sample are compared to the performance with 10 nm and additional 20 nm Cr-layers deposited on the sample surfaces. Oxidation and reduction experiments were performed in the interval $0.10 \leq p(O_2)/\text{bar} \leq 0.15$. The lines are guides for the eye.

2.3. XPS analyses

The chemical composition of the near surface regions as well as the bulk of the fresh and the degraded samples was characterized by X-ray photoelectron spectroscopy (XPS). The investigations were performed at room temperature in ultra-high vacuum (base pressure 2×10^{-10} mbar) utilizing a Thermo MultiLab 2000 spectrometer with an alpha 110 hemispherical analyzer (Thermo Electron), operated in the constant analyzer energy mode with a pass energy of 100 eV. The spectra were acquired using Al Kα radiation (1486.6 eV) monochromatized by a twin crystal monochromator yielding a focused X-ray spot 500 μm in diameter. The areas of the detected XPS peaks in the survey spectra were used to evaluate the chemical composition after a background subtraction was performed and experimentally calibrated sensitivity factors for each element were taken into account. An EX05 Ion Gun (Thermo Electron) providing a 3 keV Ar-ion beam was used for the acquisition of elemental depth profiles. The surface area irradiated at an ion current of approximately 3 μA was 1.5 mm × 1.5 mm.

3. Results and discussion

3.1. Oxygen exchange kinetics

The effect of chromium poisoning on the long-term stability of the chemical oxygen surface exchange coefficient at 600 °C is shown in Figs. 1 and 2. For the fresh samples, high values of k_{chem}, i.e. 3.0×10^{-5} cm s^{-1} (LSC) and 2.7×10^{-6} cm s^{-1} (NDN), are obtained, which remain stable during 200–300 h of testing. Subsequently, after the deposition of a 10 nm thick Cr-layer onto the sample surfaces, k_{chem} of LSC decays by a factor of about 2 and remains constant at 1.5×10^{-5} cm s^{-1} during 250 h of testing. When an additional 20 nm of Cr is added to the surface of LSC, k_{chem} decreases again by a factor of 2 to $k_{chem} = 8.0 \times 10^{-6}$ cm s^{-1}, i.e. 27% of the initial performance. In agreement with a similar study on LSCF [37], a clear dependence of the deterioration of the chemical surface oxygen exchange coefficient on the Cr-layer thickness is observed.

For the fresh LSC-sample, as well as that with a 10 nm Cr-layer, it was also possible to obtain values for the chemical diffusion coefficient of oxygen D_{chem}. As expected, chromium poisoning mainly affects k_{chem}, whereas the degradation of the bulk diffusion coef-

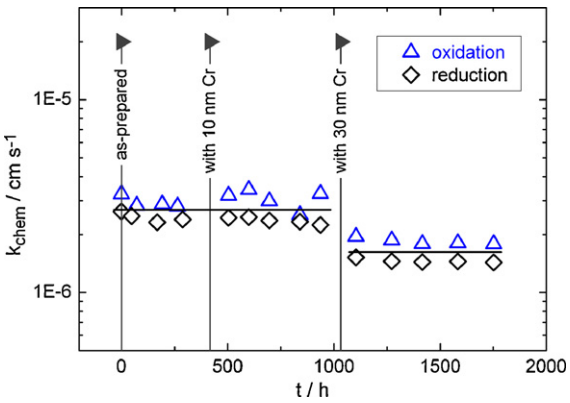

Fig. 2. Decrease of the chemical oxygen surface exchange coefficient k_{chem} of NDN due to chromium poisoning at 600 °C. Data of the fresh sample are compared to the performance with 10 nm and additional 20 nm Cr-layers deposited on the sample surfaces. Oxidation and reduction experiments were performed in the interval $0.10 \leq p(O_2)/\text{bar} \leq 0.15$. The lines are guides for the eye.

ficient due to the application of a 10 nm thick Cr-layer is almost negligible, i.e. the performance remains at about 80% of the initial value [38]. As a result of the significant decrease of k_{chem} after the application of an additional 20 nm of chromium, D_{chem} could not be evaluated, since the kinetics is exclusively rate-controlled by the surface exchange process.

In comparison to LSC, a much higher stability of NDN towards chromium poisoning is observed, as shown in Fig. 2. The effect of a Cr-layer of 10 nm thickness on the surface exchange coefficient is below the resolution of the experimental method, i.e. $k_{chem} = 2.7 \times 10^{-6}\,\text{cm s}^{-1}$ remains stable at the level of the untreated sample for 1000 h of testing. Finally, after the application of an additional 20 nm of chromium on NDN, a minor decrease of k_{chem} (by a factor less than 2) is observed. In the case of NDN, no data for the chemical diffusion coefficient of oxygen could be determined, since the kinetics is in the surface-controlled regime.

In order to be able to analyze the oxygen exchange properties from the conductivity relaxation experiments within reasonable time scales (e.g. one day for the oxidation and one day for the reduction process) thin samples of LSC and NDN were required, as stated in Section 2.1. Since, with these specimen, the kinetics was in most cases surface exchange-controlled (see above), the decrease of k_{chem} shortly after the Cr-layers were applied allowed to detect the inhibition of the oxygen surface exchange process by Cr-poisoning with high accuracy. However, it is conceivable that the decrease of the bulk diffusion coefficient could become significant with increasing penetration depth of chromium after extended periods of testing beyond the presently applied 1000 h.

Furthermore, as Cr-poisoning in the SOFC is assumed to occur via gas phase transport from an external source towards the cathode, various factors such as the amount of chromium accumulated on the cathode surface, the rate of its chemical reaction as well as Cr-diffusion into the bulk will contribute to the overall Cr-poisoning process. Considering that the oxidant (air) contains a certain amount of humidity, yet another factor may accelerate the decrease of k_{chem}. As previously shown, e.g. with LSCF [14] and NDN [39], a H_2O(g)-induced degradation occurs in wet atmosphere without any addition of Cr. Besides all this, the complex interplay between the kinetic parameters (k_{chem}, D_{chem}) and the microstructure (geometry) of a porous electrode has to be taken into account in order to fully understand the interference of chromium with the oxygen reduction reaction at the cathode. Thus, a general explanation of the Cr-poisoning process of a SOFC cathode is beyond the scope of this paper.

3.2. Elemental depth profiles

In order to obtain further insight into the origin of the observed degradation due to chromium poisoning, elemental depth profiles of the fresh and the degraded samples were acquired. Fig. 3(a) and (b) shows the XPS analyses of the fresh LSC sample and of LSC after 1250 h of testing at 600 °C with up to 30 nm thick Cr-layers. The as-prepared sample of LSC shows strong Sr-enrichment, but only in a very thin zone of about 1 nm. Below this layer, a constant composition is reached which can be attributed to the bulk. In comparison, the most striking feature in terms of the surface cation composition of the degraded LSC sample is the elevated Sr-content down to a much higher depth of approximately 30 nm. This zone corresponds to the thickness of the originally applied Cr-layers. As indicated by the pronounced gradients and similar profiles of the Sr- and Cr-signals, a significant cation diffusion seems to occur. At depths of >50 nm the bulk (nominal) composition of LSC is reached and the Cr-concentration becomes negligible. The effect of superficial Sr-enrichment has previously been reported for a number of comparable cathode materials [40–44]. In a systematical XPS analysis, van der Heide [41] demonstrated that even the surfaces of various freshly prepared transition metal perovskites containing La and Sr exhibit a Sr-enrichment by a factor of 1.2–2. According to the literature, progressive Sr-enrichment occurs during SOFC operating conditions and has a detrimental effect on cathode performance [42–44]. In agreement with the present experimental results, Sr-segregation has been shown to act as a driving force for Cr-poisoning of similar perovskite cathodes containing Co and Fe by forming a Sr-chromate [44–47].

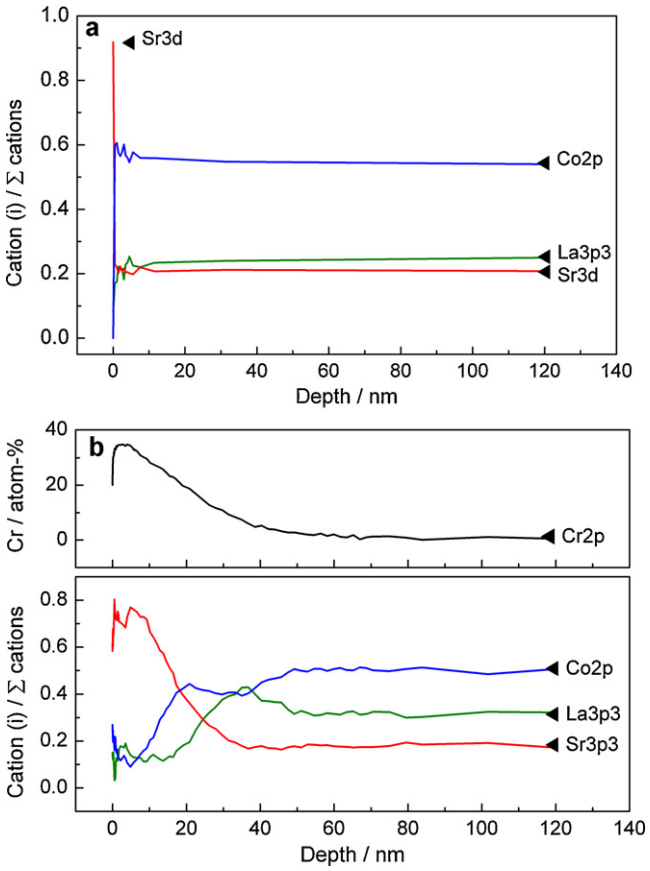

Fig. 3. (a) XPS analysis of the fresh LSC sample. (b) Post-test XPS analysis of LSC after long-term degradation at 600 °C (total test time: 1250 h; total Cr-layer thickness 30 nm).

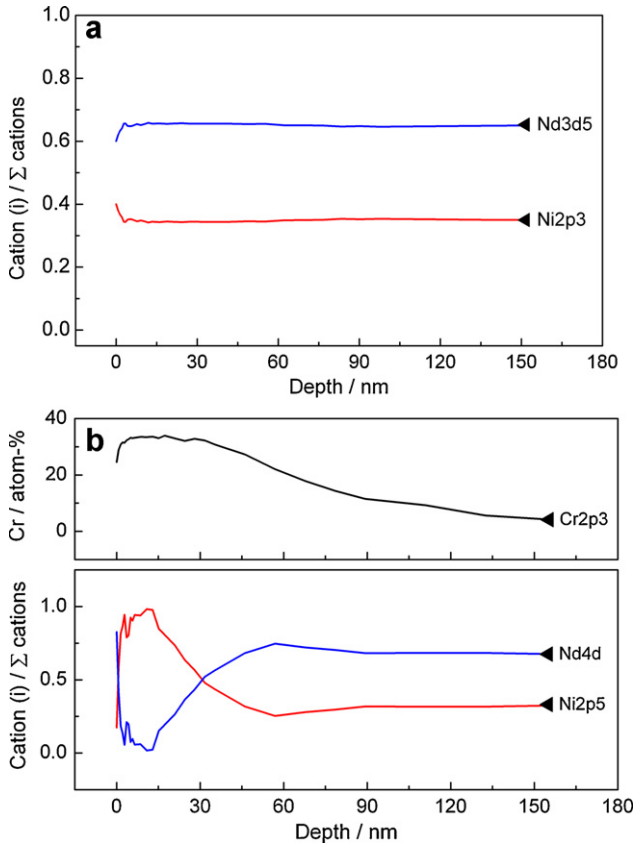

Fig. 4. (a) XPS analysis of the fresh NDN sample. (b) Post-test XPS analysis of NDN after long-term degradation at 600 °C (total test time: 1750 h; total Cr-layer thickness 30 nm).

In Fig. 4(a) and (b) the XPS depth profiles acquired on the Sr-free cathode material NDN before and after a long-term investigation at 600 °C (1750 h, with a Cr-layer of 30 nm total thickness) are shown, respectively. The as-prepared sample of NDN exhibits only small deviations from the nominal composition, i.e. a minor Nd-depletion and a small Ni-enrichment in a depth below 3 nm. The XPS analysis of the degraded NDN sample shows that, except for the first few nanometers, the Cr-rich surface zone exhibits a relatively constant Cr-content up to a depth of 30 nm, where Ni is enriched with respect to the bulk composition, while Nd is depleted. A gradient of Cr is observed over an intermediate region of 30–100 nm until the bulk composition of NDN is reached. Apart from the first 50 nm of the degraded sample, the deviations from the nominal Nd/Ni-ratio are almost negligible. The formation of a Cr-rich zone at the surface (0–30 nm) containing Ni and a certain degree of Cr-diffusion down to a depth of 50–100 nm seems to have only a minor effect on k_{chem}. To the authors' knowledge, no similar studies on NDN are available in the literature. However, the present results correspond well to previous investigations on the Sr-free nickelate $LaNi_{0.6}Fe_{0.4}O_3$ (LNF). Even though degraded LNF exhibits a certain degree of Ni-segregation with the subsequent formation of a Ni-chromate, the effect on the cathode performance was reported to be negligible [24,47,48].

4. Conclusions

Within this study it was possible to measure high k_{chem}-values for the as-prepared LSC and NDN at 600 °C. The perovskite cathode LSC containing Sr already exhibits a significant decrease of k_{chem} by a factor 2 after deposition of a 10 nm thick Cr-layer. When the thickness of Cr on LSC is increased to 30 nm, the surface exchange coefficient decreases again by a factor of 2.

In contrast to LSC the Sr-free K_2NiF_4-type cathode material NDN shows a significantly higher tolerance towards Cr-poisoning. The effect of a 10 nm thick Cr-layer on the oxygen surface exchange coefficient of the as-prepared NDN is below the detection limit of the experimental method. Even after an additional deposition of 20 nm of chromium onto NDN, the decrease of k_{chem} is below 50%. Post-test XPS analyses provided a deeper insight into the mechanisms of degradation. In the case of LSC, the significant decrease of k_{chem} due to Cr-poisoning could be correlated to the formation of a Sr-containing chromate within a depth of about 30 nm. The XPS analysis of the degraded NDN revealed a thin Cr-rich zone containing Ni (about 30 nm) and a certain degree of diffusion of Cr into a depth of 50–100 nm, which ultimately had only a minor influence on the surface exchange properties.

It should be mentioned that at 600 °C, k_{chem} of the fresh LSC sample is higher than that of NDN by a factor of 10. However, in terms of the progressive decrease in k_{chem} of LSC (equivalent to an increase in ASR) with increasing Cr-layer thickness, the material can be expected to degrade significantly during IT-SOFC operation in the presence of potential chromium sources (metal interconnects etc.) over the targeted life-spans of 5000 h for mobile SOFC applications or 40,000 h for stationary SOFCs. Thus, due to their stable performance and their high tolerance towards Cr-poisoning, Sr-free cathodes such as NDN are promising materials for IT-SOFC cathodes. Further studies on the stability of other Sr-free cathode materials and those containing Sr, with respect to Cr-poisoning are currently underway in order to evaluate the observed trends.

Acknowledgements

Financial support by the EC within the integrated project SOFC600 under Contract No. 020089 is gratefully acknowledged. In addition, the authors would like to thank J.M. Bassat of CNRS Bordeaux (France) and F. van Berkel of ECN (The Netherlands) for providing NDN and LSC pellets within the EC project SOFC600 as well as F. Klauser and E. Bertel of the University of Innsbruck (Austria) for assistance with the XPS measurements.

References

[1] Y. Teraoka, H.M. Zhang, K. Okamoto, N. Yamazoe, Mater. Res. Bull. 23 (1988) 51–58.
[2] J. Mizusaki, Solid State Ionics 52 (1992) 79–91.
[3] L.-W. Tai, M.M. Nasrallah, H.U. Anderson, D.M. Sparlin, S.R. Sehlin, Solid State Ionics 76 (1995) 259–271.
[4] L.-W. Tai, M.M. Nasrallah, H.U. Anderson, D.M. Sparlin, S.R. Sehlin, Solid State Ionics 76 (1995) 273–283.
[5] C. Sun, R. Hui, J. Roller, J. Solid State Electrochem. 14 (2010) 1125–1144.
[6] A. Tarancón, M. Burriel, J. Santiso, S.J. Skinner, J.A. Kilner, J. Mater. Chem. 20 (2010) 3799–3813.
[7] C. Peters, A. Weber, E. Ivers-Tiffée, J. Electrochem. Soc. 155 (2008) B730–B737.
[8] J. Januschewsky, M. Ahrens, A. Opitz, F. Kubel, J. Fleig, Adv. Funct. Mater. 19 (2009) 3151–3156.
[9] A. Heel, P. Holtappels, T. Graule, J. Power Sources 195 (2010) 6709–6718.
[10] E. Bucher, A. Egger, G.B. Caraman, W. Sitte, J. Electrochem. Soc. 155 (2008) B1218–B1224.
[11] H. Yokokawa, N. Sakai, T. Horita, K. Yamaji, M.E. Brito, H. Kishimoto, J. Alloys Compd. 452 (2008) 41–47.
[12] L. Dieterle, D. Bach, R. Schneider, H. Störmer, D. Gerthsen, U. Guntow, E. Ivers-Tiffée, A. Weber, C. Peters, H. Yokokawa, J. Mater. Sci. 43 (2008) 3135–3143.
[13] P. Hjalmarsson, M. Søgaard, M. Mogensen, Solid State Ionics 179 (2008) 1422–1426.
[14] E. Bucher, W. Sitte, Solid State Ionics, in press, doi:10.1016/j.ssi.2010.01.006.
[15] F. Mauvy, C. Lalanne, J.M. Bassat, J.C. Grenier, H. Zhao, P. Dordor, P. Stevens, J. Eur. Ceram. Soc. 25 (2005) 2669–2672.
[16] H. Zhao, F. Mauvy, C. Lalanne, J.M. Bassat, S. Fourcade, J.C. Grenier, Solid State Ionics 179 (2008) 2000–2005.
[17] A. Egger, E. Bucher, W. Sitte, C. Lalanne, J.M. Bassat, in: S.C. Singhal (Ed.), Proc. of the 11th Int. Symp. Solid Oxide Fuel Cells (SOFC-XI), Vienna, Austria, 2009, pp. 2547–2556.
[18] M. Greenblatt, Curr. Opin. Solid State Mater. Sci. 2 (1997) 174–183.

[19] H. Tamura, H. Hayashi, Y. Ueda, Physica C 258 (1996) 61–71.
[20] E. Boehm, J.M. Bassat, P. Dordor, F. Mauvy, J.C. Grenier, P. Stevens, Solid State Ionics 176 (2005) 2717–2725.
[21] E.N. Naumovich, M.V. Patrakeev, V.V. Kharton, A.A. Yaremchenko, D.I. Logvinovich, F.M.B. Marques, Solid State Sci. 7 (2005) 1353–1362.
[22] C. Lalanne, G. Prosperi, J.M. Bassat, F. Mauvy, S. Fourcade, P. Stevens, M. Zahid, S. Diethelm, J. Van Herle, J.C. Grenier, J. Power Sources 185 (2008) 1218–1224.
[23] V.A.C. Haanappel, C. Lalanne, A. Mai, F. Tietz, J. Fuel Cell Sci. Technol. 6 (2009) 0410161–04101616.
[24] T. Komatsu, R. Chiba, H. Arai, K. Sato, J. Power Sources 176 (2008) 132–137.
[25] S.P. Jiang, Y.D. Zhen, Solid State Ionics 179 (2008) 1459–1464.
[26] H. Yokokawa, in: W. Vielstich, H. Yokokawa, H.A. Gasteiger (Eds.), Handbook of Fuel Cells – Fundamentals, Technology and Applications, John Wiley & Sons, Ltd., 2009, pp. 923–932.
[27] N.H. Menzler, A. Mai, D. Stöver, in: W. Vielstich, H. Yokokawa, H.A. Gasteiger (Eds.), Handbook of Fuel Cells – Fundamentals, Technology and Applications, John Wiley & Sons, Ltd., 2009, pp. 566–578.
[28] J.A. Schuler, C. Gehrig, Z. Wuillemin, A.J. Schuler, J. Wochele, C. Ludwig, A. Hessler-Wyser, J. Van Herle, in: P. Connor (Ed.), Proc. of the 9th European Solid Oxide Fuel Cell Forum, Lucerne, Switzerland, 2010, pp. 7111–7127.
[29] X. Montero, F. Tietz, D. Sebold, H.P. Buchkremer, A. Ringuede, M. Cassir, A. Laresgoiti, I. Villarreal, J. Power Sources 184 (2008) 172–179.
[30] P.D. Jablonski, D.E. Alman, J. Power Sources 180 (2008) 433–439.
[31] S.-H. Kim, J.-Y. Huh, J.-H. Jun, J.-H. Jun, J. Favergeon, Curr. Appl. Phys. 10 (2010) S86–S90.
[32] D. Chatterjee, S. Biswas, Int. J. Hydrogen Energy, in press, doi:10.1016/j.ijhydene.2010.04.114.
[33] Q.X. Fu, D. Sebold, F. Tietz, H.P. Buchkremer, Solid State Ionics, in press, doi:10.1016/j.ssi.2010.03.010.
[34] A. Douy, Int. J. Inorg. Mater. 3 (2001) 699–707.
[35] W. Preis, E. Bucher, W. Sitte, Solid State Ionics 175 (2004) 393–397.
[36] E. Bucher, A. Egger, P. Ried, W. Sitte, P. Holtappels, Solid State Ionics 179 (2008) 1032–1035.
[37] M. Finsterbusch, A. Lussier, E. Negusse, Z. Zhu, R.J. Smith, J.A. Schaefer, Y.U. Idzerda, Solid State Ionics 181 (2010) 640–645.
[38] M. Yang, E. Bucher, W. Sitte, in: P. Connor (Ed.), Proc. of the 9th European Solid Oxide Fuel Cell Forum, Lucerne, Switzerland, 2010, pp. 10151–10155.
[39] A. Egger, W. Sitte, F. Klauser, E. Bertel, J. Electrochem. Soc. 157 (2010) B1537–B1541.
[40] J.A. Marcos, R.H. Buitrago, E.A. Lombardo, J. Catal. 105 (1987) 95–106.
[41] P.A.W. van der Heide, Surf. Interface Anal. 33 (2002) 414–425.
[42] S.P. Simner, M.D. Anderson, M.H. Engelhard, J.W. Stevenson, Electrochem. Solid-State Lett. 9 (2006) A478–A481.
[43] S. Fearn, J. Rossiny, J. Kilner, Solid State Ionics 179 (2008) 811–815.
[44] D. Oh, E. Armstrong, D. Jung, C. Kan, E. Wachsman, in: S.C. Singhal (Ed.), Proc. of the 11th Int. Symp. Solid Oxide Fuel Cells (SOFC-XI), Vienna, Austria, 2009, pp. 2871–2879.
[45] S.P. Jiang, S. Zhang, Y.D. Zhen, J. Electrochem. Soc. 153 (2006) A127–A134.
[46] E. Konysheva, H. Penkalla, E. Wessel, J. Mertens, U. Seeling, L. Singheiser, K. Hilpert, J. Electrochem. Soc. 153 (2006) A765–A773.
[47] H. Yokokawa, T. Horita, N. Sakai, K. Yamaji, M.E. Brito, Y.P. Xiong, H. Kishimoto, Solid State Ionics 177 (2006) 3193–3198.
[48] T. Komatsu, H. Arai, R. Chiba, K. Nozawa, M. Arakawa, K. Sato, Electrochem. Solid-State Lett. 9 (2006) A9–A12.